Coexistence of Magnetism and Superconductivity in $EuFe_2As_2$ under Pressure

We have investigated the relationship between magnetism and superconductivity in the FeAs-based superconductor $EuFe_2As_2$ under pressure by measuring the ^{57}Fe nuclear forward scattering (NFS). The antiferromagnetic order in the Fe sublattice coexists microscopically with bulk superconductivity in the pressure range from 2.4 GPa to 3.0 GPa. The spectral features of ^{57}Fe NFS change markedly between the superconducting state at 2.7 GPa and the normal conducting states below 1.9 GPa, indicating modulation of the direction of the magnetic hyperfine field in the Fe sublattice. These results demonstrate the intriguing interplay between magnetism and superconductivity in Fe-based superconductors.

The coexistence between magnetism and superconductivity has aroused great interest in the pairing mechanisms in novel superconductors. Among these novel superconductors, the FeAs-based superconductors AFe_2As_2 (A: Sr, Ba, and Eu) have attracted much attention for the coexistence phases with strong interplays among magnetism, structure, and superconductivity [1].

AFe_2As_2 with a tetragonal structure shows an antiferromagnetic order at T_o^{Fe} = 140–200 K with the structural change to an orthorhombic one [2, 3]. In the case of $EuFe_2As_2$, the Eu^{2+} magnetic moments order antiferromagnetically at T_o^{Eu} = 19 K [4]. The magnetic structure of the Fe sublattice at ambient pressure is the stripe antiferromagnetic (sAFM) one and these magnetic moments are aligned along [100] in the orthorhombic structure [4, 5]. The T_o^{Fe} value is sufficiently suppressed by pressure or substitution, and then bulk superconductivity emerges at low temperature [6–8]. The microscopic coexistences of a long-range magnetic order and superconductivity have been observed in underdoped regions of these substituted AFe_2As_2 superconductors [7–10]. Theoretically, it was predicted using a weak-coupling itinerant model that magnetic states in the coexistence phases are strongly influenced by disorders in compounds due to substitutions [11]. Thus, it is important to investigate the interplay between magnetism and superconductivity of AFe_2As_2 under pressure because hydrostatic pressure controls the electronic state of a material without introducing any disorders. In this article, we report on the magnetic state with superconductivity in $EuFe_2As_2$ under pressure via the ^{57}Fe nuclear forward scattering (NFS).

^{57}Fe NFS experiments under high pressure at low temperatures were carried out using a clamp-type diamond anvil cell (DAC) on the AR-NE1. The [001] of the single-crystalline sample in DAC was aligned along the propagation vector $\boldsymbol{k}_0$ of the incident X-ray.

Figure 1(a) shows the pressure–temperature phase diagram evaluated by the ^{57}Fe NFS and dc magnetic susceptibility under pressure. The T_o^{Fe} value steeply decreases with increasing pressure and then disappears around 3 GPa, whereas the T_o^{Eu} value gradually increases with no anomaly up to 5 GPa. Superconductivity was observed below T_{sc} ~ 25 K in the pressure range from p_c^L ~ 2.4 to p_c^H ~ 3.0 GPa [6].

Typical ^{57}Fe NFS spectra at 4 K are shown in Figs. 1(b) and (c). The observed high-frequency quantum beats (QBs) arise from the energy splitting in the nuclear levels by the magnetic hyperfine field H_{hf}^{Fe} in the magnetic order: they verify a long-range magnetic order in the Fe sublattice of $EuFe_2As_2$ below p_c^H at 4 K. Note that the features of QBs in the spectrum at 2.7 GPa (>p_c^L) are much different from that at 1.9 GPa (<p_c^L). Especially, the minima at around 80 and 150 ns in the ^{57}Fe NFS spectrum at 1.9 GPa become shallower than that at 2.7 GPa, as indicated by arrows in Figs. 1(b) and (c). At 2.7 GPa, these shallow minima become deeper with increasing temperature and then the spectral features at 46 K (>T_{sc}) are similar to that at 4 K and 1.9 GPa [Figs. 1(b) and (d)]. These differences in the features of QBs indicate that the magnetic order in the Fe sublattice changes in the superconducting phase.

Since the incident photons are perfectly σ-polarized radiations, the features of QBs in the ^{57}Fe NFS spectra depend on $\boldsymbol{H}_{hf}^{Fe}$ and the principal axes of the diagonalized EFG tensor relative to $\boldsymbol{k}_0$. The local environment around the Fe site in the orthorhombic structure is similar to that with $\bar{4}m2$ in the tetragonal structure [2]. Thus, we assume that the diagonalized EFG tensor has axial symmetry and the principal z-axis is parallel to [001] under pressure at low temperatures. As shown in Figs. 1(b) and (d), the ^{57}Fe NFS spectra in the normal-conducting phase are well analyzed by assuming the sAFM structure ($\boldsymbol{H}_{hf}^{Fe}$ // [100]) with a structural twinning effect. However, the ^{57}Fe NFS spectrum at 2.7 GPa is not described either by the sAFM structure or by magnetically ordered and paramagnetic Fe states. To analyze the spectrum at 2.7 GPa and 4 K, we need three spectroscopically nonequivalent Fe sites with different directions of H_{hf}^{Fe}, indicating the directional modulation of the Fe moments from the sAFM state. As shown in Fig. 1(c), the observed spectrum was reproduced using this assumption with no structural twinning effect. Consequently, the magnetic structure of the Fe sublattice with superconductivity differs from the sAFM one, demonstrating the intriguing relationship between magnetism and superconductivity in $EuFe_2As_2$ under pressure.

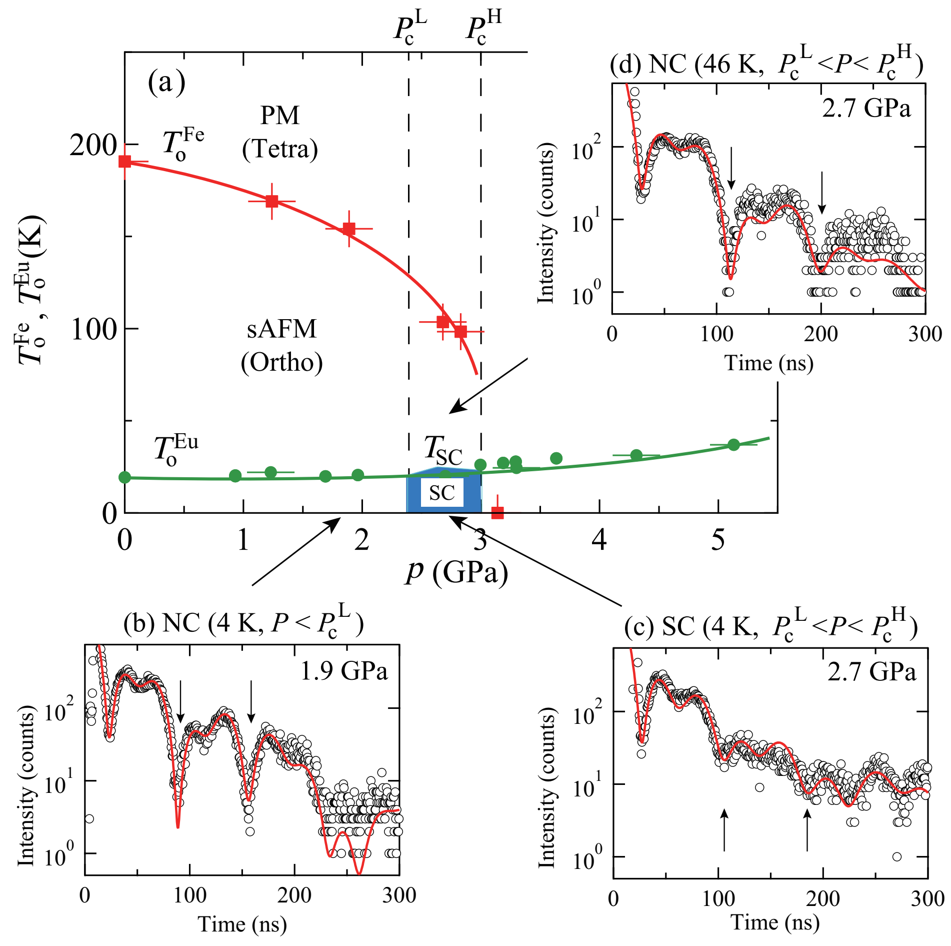

Figure 1: (a) Pressure-temperature phase diagram and (b–d) typical ^{57}Fe nuclear forward scattering spectra of $EuFe_2As_2$ under pressure. The blue area in (a) represents the superconducting phase. The red lines in (b–d) show the results of fitting.

REFERENCES

[1] E. Abrahams and Q. Si, *J. Phys.: Condens. Matter* **23**, 223201 (2011).
[2] M. Tegel, M. Rotter, V. Weiß, F. M. Schappacher, R. P öttgen and D. Johrendt, *J. Phys.: Condens. Matter* **20**, 452201 (2008).
[3] M. Rotter, M. Tegel, D. Johrendt, I. Schellenberg, W. Hermes and R. Pöttgen, *Phys. Rev. B* **78**, 020503(R) (2008).
[4] Y. Xiao, Y. Su, M. Meven, R. Mittal, C. M. N. Kumar, T. Chatterji, S. Price, J. Persson, N. Kumar, S. K. Dhar, A. Thamizhavel and Th. Brueckel, *Phys. Rev. B* **80**, 174424 (2009).
[5] K. Kaneko, A. Hoser, N. Caroca-Canales, A. Jesche, C. Krellner, O. Stockert and C. Geibel, *Phys. Rev. B* **78**, 212502 (2008).
[6] N. Kurita, M. Kimata, K. Kodama, A. Harada, M. Tomita, H. S. Suzuki, T. Matsumoto, K. Murata, S. Uji and T. Terashima, *Phys. Rev. B* **83**, 214513 (2011).
[7] F. Waßer, A. Schneidewind, Y. Sidis, S. Wurmehl, S. Aswartham, B. Büchner and M. Braden, *Phys. Rev. B* **91**, 060505(R) (2015).
[8] J. M. Allred, K. M. Taddei, D. E. Bugaris, M. J. Krogstad, S. H. Lapidus, D. Y. Chung, H. Claus, M. G. Kanatzidis, D. E. Brown, J. Kang, R. M. Fernandes, I. Eremin, S. Rosenkranz, O. Chmaissem and R. Osborn, *Nat. Phys.* **12**, 493 (2016).
[9] E. Wiesenmayer, H. Luetkens, G. Pascua, R. Khasanov, A. Amato, H. Potts, B. Banusch, H.-H. Klauss and D. Johrendt, *Phys. Rev. Lett.* **107**, 237001 (2011).
[10] W. T. Jin, S. Nandi, Y. Xiao, Y. Su, O. Zaharko, Z. Guguchia, Z. Bukowski, S. Price, W. H. Jiao, G. H. Cao and Th. Brückel, *Phys. Rev. B* **88**, 214516 (2013).
[11] M. Hoyer, R. M. Fernandes, A. Levchenko and J. Schmalian, *Phys. Rev. B* **93**, 144414 (2016).

BEAMLINE

AR-NE1

S. Ikeda[1], Y. Tsuchiya[1], X. W. Zhang[2], S. Kishimoto[2], T. Kikegawa[2], Y. Yoda[3], H. Nakamura[4], M. Machida[4], J. K. Glasbrenner[5] and H. Kobayashi[1] ([1]Univ. of Hyogo, [2]KEK-IMSS-PF, [3]JASRI, [4]JAEA, [5]U.S. NRL)